Available online at www.sciencedirect.com
ScienceDirect
Biochimica et Biophysica Acta 1768 (2007) 1036–1049
Biochimica et Biophysica Acta
BBA
www.elsevier.com/locate/bbamem

Distribution of reaction products in phospholipase A_2 hydrolysis

Hanna P. Wacklin [a,*,1], Fredrik Tiberg [b], Giovanna Fragneto [c], Robert K. Thomas [a]

[a] *Oxford University, Physical and Theoretical Chemistry Laboratory, South Parks Road, Oxford OX1 3QZ, UK*
[b] *Camurus AB, Ideon Science Park, Gamma 2, SE-223 70 Lund, Sweden*
[c] *Institut Laue-Langevin, 6 rue Jules Horowitz, BP 156, 38042 Grenoble, France*

Received 30 May 2006; received in revised form 20 September 2006; accepted 30 October 2006
Available online 10 November 2006

Abstract

We have monitored the composition of supported phospholipid bilayers during phospholipase A_2 hydrolysis using specular neutron reflection and ellipsometry. Porcine pancreatic PLA_2 shows a long lag phase of several hours during which the enzyme binds to the bilayer surface, but only 5±3% of the lipids react before the onset of rapid hydrolysis. The amount of PLA_2, which resides in a 21±1 Å thick layer at the water-bilayer interface, as well as its depth of penetration into the membrane, increase during the lag phase, the length of which is also proportional to the enzyme concentration. Hydrolysis of a single-chain deuterium labelled d_{31}-POPC reveals for the first time that there is a significant asymmetry in the distribution of the reaction products between the membrane and the aqueous environment. The lyso-lipid leaves the membrane while the number of PLA_2 molecules bound to the interface increases with increasing fatty acid content. These results constitute the first direct measurement of the membrane structure and composition, including the location and amount of the enzyme during hydrolysis. These are discussed in terms of a model of fatty-acid mediated activation of PLA_2.

Keywords: Phospholipase A_2; Lag phase; Lyso-lipid; Fatty acid; Supported bilayer; Neutron reflection

1. Introduction

Phospholipase A_2 (PLA_2) selectively cleaves the *sn*-2 ester bonds in 3-*sn*-phosphoglyceride lipids, the main lipid component of mammalian cell membranes. PLA_2 is present in a wide range of biological environments from invertebrate and insect venoms to the mammalian immune system [1], and performs a large number of different physiological functions, although the chemistry at its catalytic site is preserved across species and class. The atomic resolution structures of many PLA_2s [2] have established a catalytic mechanism [3,4], in which a His-Asp pair or a Serine residue participate in the transition state resulting from hydrolytic attack by water. In contrast to enzymes that operate in solution, PLA_2 only catalyses hydrolysis in the presence of an aggregated lipid interface, and is therefore an interfacially activated enzyme [5].

Pancreatic PLA_2 exhibits a long lag period in zwitterionic phosphocholine membranes before the onset of hydrolysis [6], and its biological function is to digest lipids in bile salts (negatively charged), whereas most venom PLA_2s are highly active towards neutral lecithin (mammalian cell) membranes. Non-pancreatic secreted PLA_2s in the immune system are also activated by negative charge [7,8]. Recently it has been found that the burst of hydrolysis coincides with the maximum available membrane edge in supported membranes [9] and also with the maximum in lateral membrane heterogeneity that accompanies the lipid main phase transition [10]. Perhaps the most intriguing result is that there appears to be a critical fraction of the hydrolysis products (0.083) that is required for the onset of rapid hydrolysis [11]. Apart from membrane heterogeneity, the suggested mechanisms of PLA_2 activation to explain the lag phase include slow penetration of the enzyme into the membrane [12], a membrane-induced conformational change of the enzyme into a catalytically active form [13], dimerisation of the enzyme

Abbreviations: d_{31}-POPC, L-α-1-*O*-d_{31}-palmitoyl,2-*O*-oleyl,3-*O*-*sn*-glycerophosphocholine; PLA_2, phospholipase A_2; DOPC, L-α-1,2-*O*-dioleyl-3-*O*-*sn*-glycerophosphocholine; DPPC, L-α-1,2-*O*- palmitoyl-3-*O*-*sn*-glycerophosphocholine; DDM, n-β-D-docecyl maltoside

* Corresponding author.
E-mail address: hanna.wacklin@ansto.gov.au (H.P. Wacklin).
[1] Present address: Australian Nuclear Science and Technology Organisation, Institute for Environmental Research, PMB1 Menai, NSW 2234, Australia.

0005-2736/$ - see front matter.
doi:10.1016/j.bbamem.2006.10.020

in the membrane as a pre-requisite to activation [14], and autocatalysis mediated by the reaction products [15], a fatty acid and a lyso-lipid, which are known to act as membrane permeabilisation agents [16]. Regardless of the details of the activation process, there also seems to be an auto-inhibitory feature in the mechanism of PLA_2, since the hydrolysis does not necessarily proceed to completion but can cease at a point characteristic for a given enzyme and membrane composition, with the enzyme still found to be active if an avenue of substrate replenishment is introduced [17].

Because phospholipase A_2 is a water soluble enzyme that associates with phospholipid membranes during catalysis, analysis of the reaction kinetics is complicated by the binding equilibria of the enzyme and the reaction products to the lipid interface, as illustrated in Fig. 1. The physico-chemical properties of a membrane such as fluidity, hydrophobicity, surface charge and heterogeneity are intricately linked to its molecular composition, and the accumulation of insoluble reaction products would be expected to change the nature of the membrane and the progress of catalysis. In the absence of techniques to measure interfacial composition in-situ, several experimental protocols have been developed, in which the effect of the lipid insolubility is suppressed by using either short-chain soluble lipids or detergent solubilisation [12,18,19]. Another approach has been the use of negatively charged phosphomethanol lipid analogues [20] that inhibit substrate and enzyme exchange via the solution medium and allow the substrate vesicles to be treated as independent catalytic surfaces. In both cases, heterogeneous catalysis is reduced to a two-dimensional Michaelis–Menten problem, which makes it possible to employ traditional kinetic analysis to extract most of the parameters [21,22]. However, rate measurements have largely been carried out using methods that sample the entire reaction mixture and offer no information about the relative distributions of the substrate, products or the enzyme between the catalytic interface and the surrounding solution. Surface area and pressure changes recorded for monolayers at the air–water interface have indicated that solubilisation of short-chain lipid material takes place [23], but cannot distinguish between the components at the surface. On the other hand, fluorescence microscopy has been used to monitor the morphological changes induced by hydrolysis. Both domain formation and enzyme accumulation have been found to be dependent on the chain length of the fatty acid product [24], from which it has been inferred that the enzyme is attracted to the fatty acid-rich domains. Frequency shifts in the enzyme fluorescence spectra have been used to suggest that a conformational change of the enzyme is required for catalytic activity and that there is an interaction between PLA_2 and the lipid membrane during the lag-phase [15]. Although the temperature and lipid phase transition dependence of the lag phase has been investigated by several groups, any unexplained differences in rates between different substrates have generally been combined under the heading of "interfacial quality effects".

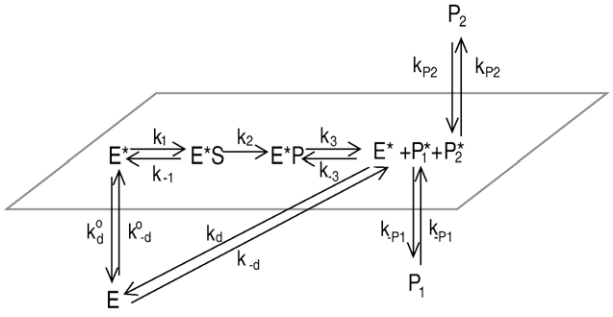

Fig. 1. A schematic model of interfacial catalysis by PLA_2. E = enzyme, * indicates a membrane bound species, S = substrate, P = products. k_i indicate the rate constants for each process. By distiguishing between k_d/k_{-d} and k_d^0/k_{-d}^0 the model takes into account any effects of hydrolysis on the membrane association/dissociation rate constants of PLA_2.

A limiting factor in the study of PLA_2 kinetics has been the lack of methods to analyse the membrane composition in situ during the reaction in order to determine the partitioning of the reaction products between the membrane and water. Likewise, methods for detecting the location and amount of PLA_2 at the membrane–water interface have not been available. We have used specular neutron reflection [25] to determine the composition of supported phospholipid model membranes during PLA_2 hydrolysis. This technique is non-destructive for biological materials, and the sensitivity of neutrons to nuclear isotopes can be used to highlight parts of the membrane using deuterium labelling of the lipids. The application of neutron reflection to biological materials and membranes [26–29] is still relatively new, but several reports have recently been published, which highlight the capabilities of this technique, including studies of new biomimetic membranes [28,30,31], membrane binding peptides [32], cholera toxin subunit B attached to a lipid monolayer [33], and the conformation of neural cell adhesion molecule NCAM [34]. Supported membranes [35] at the SiO_2–water interface are particularly good substrates for biophysical studies of membrane binding proteins due to the SiO_2–D_2O contrast, which is very sensitive to the surface coverage of the supported bilayer and the composition of the lipid hydrocarbon core. Model membrane formation from solution [36,37] allows the determination of bilayer structure and composition in-situ [28,38]. Phospholipid monolayers have also been investigated using neutron reflection [39–42], but the air–water interface requires deuteration of the lipids to obtain a reflection signal, and in such thin layers thickness and scattering length density changes are coupled in such as way as to be difficult to distinguish from each other.

Previously, we used neutron reflectivity [25] and ellipsometry [43] measurements of supported phosphocholine bilayers during *Naja mossambica mossambica* PLA_2 hydrolysis to show that the enzymatic breakdown of the lipids leads to the destruction of the supported bilayer and solubilisation of up to 90% of the lipid material [44]. The enzyme was in all cases found to reside in a 21 ± 1 Å thick layer at the lipid–water interface with partial penetration into the outer membrane leaflet, which increased with increasing lipid chain saturation. The extent of the reaction decreased with increasing chain saturation, indicating that the hydrophobic region exerts a regulating force on the enzyme, which was also supported by the strong and irreversible binding of PLA_2 to a hydrophobic self-assembled monolayer without any evidence for denaturation.

In the current paper, we present new results on membrane structure and composition determined during and after the lag phase of porcine pancreatic PLA_2. We have also for the first time used single-chain deuterium labelled d_{31}-POPC to monitor the distribution of the reaction products during both the lag phase and active hydrolysis. This lipid has a perdeuterated *sn*-1 palmitoyl (C16:0) chain and an unmodified *sn*-2 oleyl (C18:1) chain. A reaction scheme with the scattering length densities that formed the basis of our data analysis of the phosphocholine components is presented in Fig. 2. As the half-deuterated phospholipid molecules are hydrolysed by PLA_2, a deuterated lyso-lipid and a non-deuterated fatty acid are created, which allows their partitioning between the surface and the bulk solution to be monitored as changes in the scattering length density of the bilayer.

2. Materials and methods

2.1. Neutron reflection

Neutron reflection [45] measures the composition of an adsorbed layer perpendicular to the interface, and its sensitivity to the layer structure depends on the scattering contrast between the film and the surrounding media. The thickness of a thin film is related to the separation of neutron interference fringes while the amplitude of the fringes is directly proportional to the scattering length density profile (or neutron refractive index profile) of the system. The neutron scattering length density $\rho(z)$ of the system is defined in Eq. (1),

$$\rho(z) = \sum_j n_j(z) b_j \tag{1}$$

where b_j is the neutron scattering length (or power) of nucleus j and $n_j(z)$ the number of atomic nuclei in the direction perpendicular to the surface. The scattering length density is a function of the distribution of atoms per unit volume, and thus describes the composition of an adsorbed film directly. The specular reflectivity R as a function of the momentum transfer vector Q can be calculated exactly using an optical matrix model [46], which divides the surface region into homogeneous layers distinguished by their scattering length density. While model independent data fitting [47] is possible for simple interfaces, it is not well suited for analysis of reflection from complex interfaces containing multiple components, but it is often used in conjunction with more specific box models. Computer programs such as Afit (v. 3.1) [48], allow the simulation of reflectivity profiles by modelling the thickness, scattering length density, solvent volume fraction and roughness of each "box" or layer into which the interface is divided, e.g. lipid head groups and tails. Although this kind of program allows the variation of all parameters for each layer independently (thereby generating a large number of possible solutions), we used a global volume-constraint on the lipid molecules to find a unique, physically realistic solution. This procedure relies on the fundamental assumptions that (i) each lipid head group must only be connected to two hydrocarbon chains and that (ii) the number of phospholipid molecules on both sides of the bilayer must be identical within this restraint. This ensures the correct distribution of the water molecules present at the interface whilst maintaining the proportions of the lipid molecules. In other words, the thickness and solvent content of lipid chain and headgroup boxes are coupled to each other in our simulations.

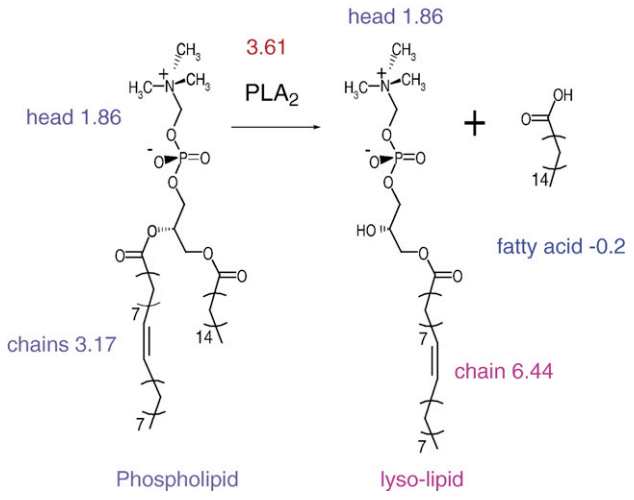

Fig. 2. Reaction scheme for phospholipid hydrolysis by PLA_2. The numbers indicated for the head groups and chains are the scattering length densities of the components in units of 10^{-6} Å^{-2}, as calculated from molecular component volumes [54].

In the case of a layer composed of a mixture of molecules, the scattering length density is the sum of the molecular scattering length densities ρ_i weighted by the volume fractions ϕ_i at which each component is present, for example in a mixture of phospholipid (l), enzyme (E) and water (w), the scattering length density will be:

$$\rho_{\text{layer}} = \phi_l \rho_l + \phi_E \rho_E + \phi_w \rho_w. \tag{2}$$

Thus, the individual volume fractions can be computed from the fitted scattering length densities of the lipid hydrocarbon core and headgroup regions, and the enzyme layer. The enzyme molecules may be considered to displace some of the lipid and/or water molecules in any of the layers in the model, subject to the constraint that the molecular proportions of the lipids and the enzyme must be conserved (e.g. the enzyme volume fractions in the layers it is present must amount to the same number of molecules across all the layers). The data analysis procedure is further explained in Materials and methods.

3. Ellipsometry

We used null ellipsometry [49] to follow the hydrolysis of phospholipid bilayers in-situ. The ellipsometric angles ψ and Δ were determined from measurement of the incident and final angles of polarisation and used to compute the complex reflection amplitude ratio ρ:

$$\rho = \left|\frac{r_p}{r_s}\right| \exp\left(\delta_{rp} - \delta_{rs}\right) = \tan\psi \exp(i\Delta) \tag{3}$$

where r_s and r_p are the reflection coefficients for s- and p-polarised light and $\delta_{rs/rp}$ represent their phase shifts upon reflection. The procedure applied to characterising the phospholipid bilayers was the same as that described by Tiberg and Landgren for surfactant films at the silica–water interface [50]. Briefly, the ellipsometric angles ψ and Δ of the bare silicon substrate are recorded in air and water (the so-called multiple-medium method) before the formation of a supported bilayer. The ellipsometric angles are related to the bilayer refractive index and to some extent, its thickness, via the Fresnel relations, which are solved numerically by requiring the refractive indices of SiO_2 and the phospholipid to be real. By using this procedure, refractive index values of $n_2 = 5.5 \pm 0.05 – 0.25 \pm 0.05\ j$ and $n_1 = 1.48 \pm 0.005$ were typically found for the bulk silicon and the silicon dioxide layer respectively. The thickness of the oxide layer was typically 270–300 Å. The bilayer surface coverage Γ (mg m^{-2}) was computed using de Feijter's Eq. (4)

$$\Gamma = \frac{(n - n_0)}{dn/dc} d \tag{4}$$

where n and n_0 are the refractive indices of the adsorbate and bulk solvent respectively, d is the adsorbed film thickness and dn/dc is the refractive index increment (0.154 for DOPC [36]) of the adsorbate(measured by classical refractometry). The standard deviation in determining the ellipsometric angles ψ and Δ was estimated previously to be of the order of 0.001° and 0.002° respectively [49]. Although the errors in thickness and refractive index can be quite large at low adsorbed amounts, they fall to less than 5% above 2 mg m^{-2}, and are coupled in a way that they cancel when the surface excess is computed. Thus the surface excess is the most reliably computed property of very thin films (<30 Å) and was our primary interest in these experiments.

3.1. Experimental procedures

Specular neutron reflection was measured on the D17 reflectometer [51] at the Institut Laue Langevin in Grenoble, France, and on SURF at ISIS, UK. Time-of-flight measurements with neutron wavelengths λ of 2–20 Å at ILL and 0.5–6 Å at ISIS were used to record reflectivity between $0.01>Q>0.3$ $Å^{-1}$, where $Q=4\pi\sin\theta/\lambda$ is the momentum transfer vector of the neutrons in the direction perpendicular to the interface. Under these conditions a typical measurement time for the full reflectivity profile was 60–70 min. The phospholipid bilayer was formed in-situ in the reflectometer sample chamber and characterised as described previously [44] prior to introduction of phospholipase A_2 at a concentration of 0.01 mg/ml. The solution was maintained at 25±0.3 °C and agitated with a magnetic flea during phospholipid adsorption. A schematic of the sample cell set up and scattering geometry is shown in Fig. 3.

Ellipsometry experiments were carried out using a Rudolph Research thin film ellipsometer type 43603–200E (horizontal reflection plane), at the University of Lund, Sweden. The angle of incidence for all measurements was ~68±0.5 °, for which a trapezoidal quartz cuvette was used to provide normal incidence to the beam. The sample cell was kept at 25±0.3 °C by a circulating water bath, and further details of the experimental set up have been published elsewhere [50].

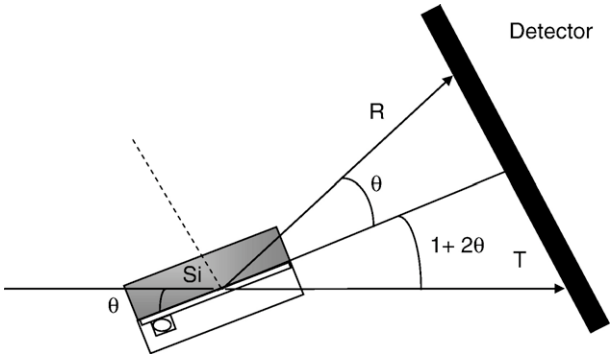

Fig. 3. Schematic model of the sample cell and reflection geometry on D17 as viewed from above. R=reflected beam, T=transmitted beam, θ=angle of incidence.

3.2. Supported bilayer formation

Phospholipid bilayers were formed by adsorption of micellar mixtures of the phospholipids with the surfactant n-β-D-dodecyl maltoside [36,37]. Gradual dilution of the bulk micellar solution leads to preferential adsorption of the phospholipid while all surfactant is removed by rinsing, leaving behind a well-characterised supported bilayer. A typical experimental procedure has 3 separate stages: characterisation of the silica-support, adsorption of the phospholipid bilayer from a 6:1 w/w mixture of β-D-dodecyl maltoside and the requisite phospholipid, and injection of 0.01 mg/ml phospholipase in buffer solution (10 mM Tris–HCl at pH 7.4). All manipulations were performed in-situ, with reflectivity/ellipsometric angles recorded before and after phospholipid adsorption and during PLA_2 hydrolysis.

3.3. Materials

d_{31}-POPC was purchased from Avanti Polar Lipids, n-β-D-dodecyl maltoside, phospholipase A_2 from *Naja mossambica mossambica* venom (P7778, ~90% purity, 1500 units per mg) and from porcine pancreas (in 1 M NH_4SO_4) were from Sigma-Aldrich and all were used as received. Ultra-high quality water (Ω=18.2 Ω) was used in all ellipsometry experiments and surface preparations. D_2O (>99%) was provided from the reactor at the Institut Laue Langevin and purchased from Sigma-Aldrich at ISIS. The support surface (Silicon (111) orientation) was polished in house, and cleaned by a 1:4:5 solution of H_2O_2:H_2SO_4:H_2O at 80 °C followed by UV ozonolysis immediately prior to the experiment, which leaves a natural oxide layer of 7–10 Å thickness and 3–5 Å roughness with 5–10% water on the surface. The solid supports for ellipsometry were prepared as described previously [44].

3.4. Data analysis

Reflectivity data were analyzed using the AFit program [48] with an optical matrix model [52] to calculate specular reflectivity. The details of this fitting procedure for supported bilayers have been previously published elsewhere [38]. In short, the phospholipid bilayer was described by a three-layer model with a uniform hydrocarbon chain between two identical head group regions. A physically realistic fit to the phospholipid bilayer reflectivity was found by requiring the water distribution to maintain the area per molecule constant throughout the bilayer to within ±3$Å^2$, which was the minimum practicable value that allowed global fitting of all the phospholipid-PLA_2 data sets. This analysis was based on the volume fractions of the lipid chain and head group components found by Petrach et al. from molecular dynamics simulations [53,54], from which the scattering length densities of phospholipid, lyso-lipid and fatty acid were calculated. The scattering length density of PLA_2 was calculated from its amino acid sequence [55,56] taking into account the exchange of hydrogens for deuteriums in polar residues [57]. The errors in bilayer structural parameters were derived from the maximum acceptable variation in the fitted

parameters, in other words the thickness, volume fraction and scattering length density of each part of the lipid bilayer. We have previously demonstrated how the sensitivity of neutron reflection to structural details can be enhanced using the volume constraint, and shown that a supported DPPC bilayer has a somewhat lower density than a bulk lamellar phase at 25 °C, and a scattering length density of 6.9×10^{-6} Å^{-1} in the palmitoyl-chain region. The reflectivity profiles from partially deuterated d_{31}-POPC -PLA_2 bilayers were fitted by allowing the lipid scattering length density to vary from that calculated for d_{31}-POPC to determine the distribution of the reaction products. The error given for the lipid scattering length density ρ is that derived from the maximum variation in this fitting parameter, while the error in the total scattering length density ρ_a (the scattering length density of layer a in the model) is also related to the error in fitting the water content of the layer and lipid volume fraction ϕ. The errors in thickness and volume fraction in the model sublayers are coupled in such a way that the total errors in surface excess and thickness are ±10% and ±2 Å respectively.

4. Results

4.1. The length of the lag phase and PLA_2 concentration

Ellipsometry was used to record the surface coverage of supported phospholipid bilayers during the course of PLA_2 hydrolysis. Fig. 4 shows the surface coverage Γ and thickness of a DOPC bilayer recorded during attack by porcine pancreatic PLA_2 at 0.01 mg/ml and 0.02 mg/ml concentrations. The point of enzyme injection is at $t=0$, and it is apparent that in both cases there is a significant induction period before the surface excess starts to decrease rapidly, which is interpreted as the onset of sustained hydrolysis. The lag period is shortened from 350 min. to 230 min. as the enzyme concentration is doubled, and at 0.02 mg/ml of PLA_2 the bilayer surface excess tends to a limiting value of 0.26 mg m^{-2} (6% of the original bilayer mass), which is nearly 3 times higher in the presence of only 0.01 mg/ml PLA_2 (0.885 mg m^{-2}, 21%).

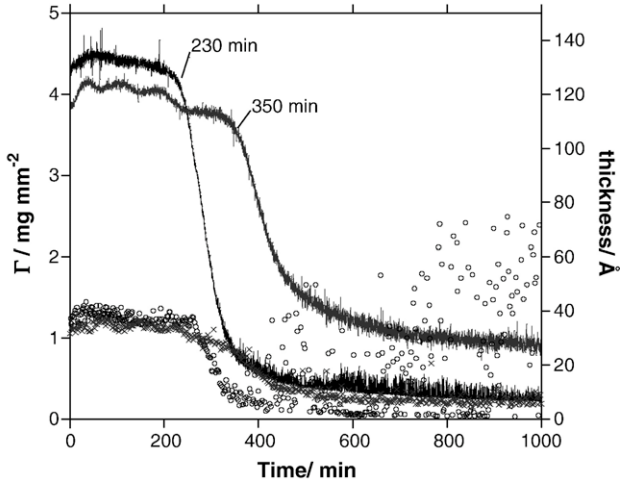

Fig. 4. Surface coverage and thickness of a DOPC bilayer recorded by ellipsometry during porcine pancreatic PLA_2 hydrolysis. 0.01 mg/ml PLA_2: (grey solid line) surface coverage Γ/mg m^{-2} and (grey crosses) bilayer thickness t/Å. 0.02 mg/ml PLA_2: (black solid line) bilayer surface coverage Γ/mg m^{-2} and (open circles) bilayer thickness t/Å. PLA_2 was injected at $t=0$ and the end of the induction period is indicated in each case.

Linear fits to the rapid phase hydrolysis after the end of the lag phase resulted in rates of 0.335 μg m^{-2} s^{-1} and 0.631 μg m^{-2} s^{-1} for 0.01 mg/ml and 0.02 mg/ml enzyme respectively, corresponding to 0.426 μmol m^{-2} s^{-1} and 0.802 μmol m^{-2} s^{-1}. In other words, doubling the enzyme concentration leads to a nearly 2-fold increase in the rate of removal of lipid from the surface, but the length of the lag phase decreases by only 34%. This implies either that not all the enzyme is immediately associated with the lipid bilayer, but accumulates during the lag period, or that, once at the interface, the enzyme molecules require a period of time to overcome an activation barrier to catalysis. It is not possible to distinguish these two mechanisms without knowledge of the location and amount of PLA_2.

The shortening of the lag phase is consistent with earlier suggestions in the literature [11] that gradual accumulation of reaction products is required to provide the ideal conditions for PLA_2 catalysis, in which case the time taken to generate a sufficient fraction of products would be shorter in the presence of a larger number of PLA_2 molecules bound to the membrane. Lateral phase separation and the presence of domain edges in the bilayer have been used to explain this autocatalytic effect of the products [10], but the negative charge of the fatty acids may also increase PLA_2 partitioning in the membrane [24].

The changes in the extent of the reaction can be understood in terms of the reduced number of enzyme molecules at the membrane interface, which, at low bilayer coverage slows down the reaction turnover. PLA_2 aggregation in fatty-acid rich regions would also act to reduce the number of active enzyme molecules in the membrane faster at lower enzyme concentration.

4.2. PLA_2 binding during the lag phase

In order to understand what changes occur in the membrane during the lag phase and how they eventually lead to a burst of enzyme activity, we recorded the neutron reflectivity profiles of phospholipid bilayers during and after the lag phase. While the small amounts of PLA_2 bound to the membranes are not detected by ellipsometry, we have previously shown that the scattering contrast in a neutron reflection measurement can be manipulated so as to yield both the amount and location of the enzyme in the phospholipid bilayer.

Fig. 5 shows the reflectivity profiles of a DOPC bilayer recorded before and after the injection of porcine pancreatic PLA_2. The results obtained from data fitting are presented in Table 1. ρ corresponds to the scattering length density of each molecular fragment, and ρ_a is used to denote the scattering length density fitted for each layer and includes any solvent present. The fitted thicknesses t of the lipid bilayer regions (heads and chains), and lipid volume fractions ϕ are given with the areas per molecule and surface coverage values Γ that were calculated from them. The surface coverage of PLA_2 denotes the total mount of PLA_2 in all the layers it was found to be present in. For example, a layer "chains+PLA2" with a 7 Å

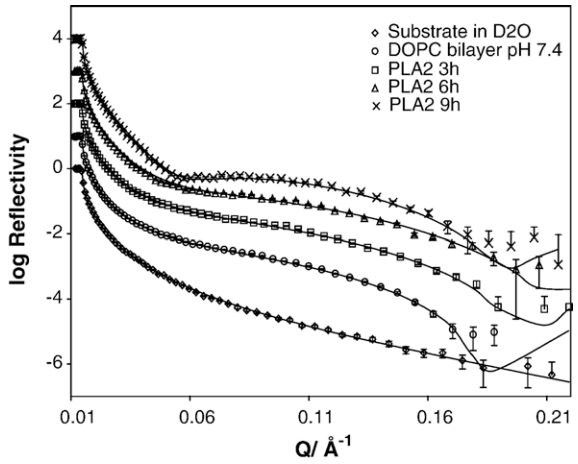

Fig. 5. Specular reflectivity of a supported DOPC bilayer at the Silica–D_2O interface recorded before and during porcine pancreatic PLA_2 hydrolysis. (Open diamonds) substrate reflectivity in D_2O, (open circles) DOPC bilayer at in 10 mM Tris–D_2O pH 7.4, (open squares) DOPC bilayer 3 h after injection of 0.01 mg/ml PLA_2, (open triangles) DOPC bilayer 6 h after PLA_2 injection and (crosses) DOPC bilayer 9 h after PLA_2 injection. The reflectivity profiles (data points) and the data fits (solid lines) have been displaced by successive factors of 10 for clarity. Statistical error bars are indicated for all data points. The data fits correspond to the bilayer parameters given in Table 1.

thickness, and "head 2+PLA2" with a 6 Å thickness denote that an increased scattering length density was found in the outer 7 Å of the chain region and the 6 Å thick outer head group region, and was assumed to be due to replacement of lipids by PLA_2. If the total thickness given for the PLA_2 layer is, for example 21 Å this indicates that the enzyme extends a further 8 Å into the solution outside the bilayer. The enzyme volume fraction denotes that the enzyme replaces this fraction of the lipids in the layer. For example 0.4 vol.% of PLA_2 in the lipid headgroup region (6 Å thick) corresponds to a volume of $0.4\times6.94\times10^{15}\times325$ Å$^3=9\times10^{17}$ Å^3, or 5.5×10^{17} Å^2 of the membrane surface area, where 6.94×10^{15} is the number of lipid molecules in the bilayer. If the total thickness of the PLA_2 layer is 21 Å, then the footprint of one PLA_2 molecule is 733 Å^2, which leads to a PLA_2 to lipid mole ratio of 0.03.

No significant changes (less than 5 v/v%) occur in the phospholipid surface coverage during the first 3 h of lipid–PLA_2 interaction, confirming the existence of a lag phase of similar length to that observed by ellipsometry. This is demonstrated by the fact that although an increase is observed in reflectivity in the $0.15>Q>0.21$ Å^{-1} region, the data could be fitted by maintaining the lipid bilayer coverage within ±10% of the original Γ. The changes in reflectivity could be modeled by describing the enzyme as occupying a 21±3 Å layer at the lipid–water interface, i.e. penetrating through the outer headgroup region and 6±3 Å into the chain region of DOPC. After 6 h, a much more pronounced change in the reflectivity shows that hydrolytic breakdown of DOPC into a lyso-lipid and fatty acid has started to cause removal of lipids from the support surface. At 9 h after enzyme injection, the destruction of the DOPC bilayer continues at a rate comparable to that previously observed for PLA_2 from *Naja mossambica mossambica* venom, with 40% of the original bilayer mass having been removed at this stage. Coincident with the start of rapid hydrolysis is also a 40% increase in membrane bound PLA_2 from 0.32 mg m^{-2} to 0.45 mg m^{-2}.

4.3. Fate of the reaction products in d_{31}-POPC hydrolysis

We also investigated the distribution of the lyso-lipid and fatty acid in *Naja mossambica mossambica* hydrolysis of d_{31}-POPC. We previously observed this enzyme hydrolyzing a supported h-POPC bilayer immediately, although at a slightly lower overall efficiency compared to DOPC. The reflectivity profiles of d_{31}-POPC before, after 70 min and after 10 h 10 min of PLA_2 hydrolysis are shown in Fig. 6. The fitting parameters and the bilayer properties calculated from the fits are summa-

Table 1
Structural parameters of DOPC bilayer measured during PLA_2 hydrolysis

Lipid	Layer	$\rho/10^{-6}$ Å^{-2}*	$\rho_a/10^{-6}$ Å^{-2}†	t/Å	ϕ	A/Å^2″	Γ/mg m^{-2}
DOPC pH 7.4	Heads	1.78±0.15	3.29±0.23	7±1	0.67±0.05	72±19	3.62±0.36
10 mM TRIS	Chains	−0.21±0.15	0.38±0.13	30±2	0.91±0.02	72±7	
pig PLA_2	Head 1	1.78±0.15	3.47±0.23	7±1	0.63±0.05	77±19	3.40±0.34
0.01 g/l 3 h	Chains	−2.1±0.15	0.12±0.13	27±2	0.95±0.02	77±8	
	Chains+PLA_2 #	0.2±0.15	0.5±0.12	6±2	0.95±0.02	77±8	
	Head 2+PLA_2 #	1.98±0.15	3.60±0.22	7±1	0.63±0.05	77±19	
	PLA_2 §	3.84±0.15	6.10±0.10	21±2	0.10±0.05	7300±3000	0.32±0.03
pig PLA_2	Head	1.78±0.15	4.02±0.23	7±1	0.51±0.05	94±26	2.76±0.28
0.01 g/l 6 h	Chains	−0.21±0.15	1.10±0.13	20±2	0.80±0.02	95±11	
	Chains+PLA_2 #	0.4±0.15	1.59±0.12	6±1	0.80±0.02	95±11	
	Head 2LA_2 #	2.09±0.15	4.18±0.21	7±1	0.51±0.05	94±26	
	PLA_2 §	3.84±0.15	5.97±0.10	20±2	0.15±0.05	5100±1400	0.45±0.05
pig PLA_2	Head 1	1.78±0.15	4.52±0.23	7±1	0.40±0.05	120±36	2.16±0.22
0.01 g/l 9 h	Chains	−0.21±0.15	2.81±0.13	24±2	0.54±0.02	122±14	
	Chains+PLA_2 #	0.4±0.15	3.14±0.12	6±2	0.54±0.02	122±14	
	Head 2+PLA_2 #	2.09±0.15	4.65±0.21	7±1	0.40±0.05	120±36	
	PLA_2 §	3.84±0.15	5.97±0.10	20±2	0.15±0.05	5100±1400	0.45±0.05

*ρ=molecular scattering length density, †ρ_a=total scattering length density of layer a. Head 1 refers to the inner headgroup layer facing the silicon surface. ″A is the area available per molecule and Γ the lipid surface excess. #PLA_2 penetrates through the outer headgroup region and 6 Å into the outer hydrocarbon region. §Molecular parameters of PLA_2 were calculated for the total thickness of this region.

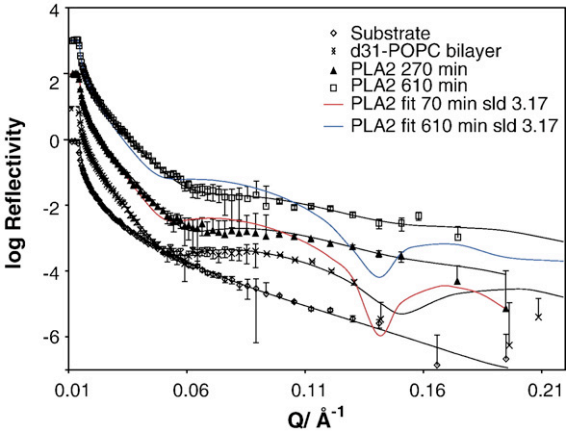

Fig. 6. Neutron reflectivity profiles (data points) from d_{31}-POPC before and during *Naja M. Mossambica* PLA_2 hydrolysis. The black lines indicate data fits from optical matrix simulations of reflectivity based on the structural parameters in Table 2. The red and blue lines are the calculated reflectivities at 70 min. and 610 min. assuming that the scattering length density of the hydrocarbon chains remains 3.17×10^{-6} Å^{-2}, i.e. both reaction products leave the interface at equal rates.

rized in Table 2, where ρ this time denotes the scattering length density fitted for each layer, including solvent. t is the thickness of each layer, assumed to be homogeneous and non-interpenetrating with neighboring layers. The data analysis was still performed using the lipid volume constraints described previously [44], but the lipid chain scattering length density was also allowed to vary to describe the effects of lipid hydrolysis with possible removal of some of the products. The bilayer initially has a lipid volume fraction of 0.82±0.05 in the hydrocarbon core region, and a thickness of 44±2 Å, with the scattering length density of the chain region found to be $3.17\pm0.15\times10^{-6}$ Å^{-2}, which is in good agreement with that calculated for a deuterated palmitoyl chain (C16:0) and an oleyl chain (C18:1), where we interpret the polar–apolar dividing surface in the molecule as occurring at the acyl carbons. From this value it is also evident that all the surfactant has been eliminated from the lipid bilayer, as its presence would lead to a decreased scattering length density in the lipid chain region ($\rho=-0.3\times10^{-6}$ Å^{-2} for the surfactant chains) and subsequently a negative error in apparent lipid volume fraction required to find a fit to the observed data.

The reflectivity changes during the entire course of hydrolysis of this lipid are very small, and are mainly indicative of membrane thinning. No minimum develops in the reflectivity profile which is characteristic of a high D_2O content. Data modeling in this situation was done following the same overall features observed during the hydrolysis on non-deuterated POPC [44]. During the first 70 min of the reaction the membrane thickness decreases to 31±2 Å, but most remarkably, the scattering length density of the lipid chain region decreases to $1.44\pm0.15\times10^{-6}$ Å^{-2}, which corresponds to a 1:3 ratio of deuterated palmitoyl chains and oleyl chains. This indicates that 50% of the lipid molecules have been hydrolyzed and that all the released d_{31}-lyso-palmitoylphosphocholine has left the interface. This also explains the small changes in reflectivity, as the scattering length density of lyso-C16:0-PC (6.44×10^{-6} Å^{-1}) is very close to D_2O. At this stage of the reaction, a 22±1 Å thick layer of the enzyme was found at the membrane–water interface in a similar position to that found in DOPC and replacing 40±5 vol.% of the outer lipid head group region. This is consistent with the amount of hydrolysed lipid (50%) indicated by the scattering length density changes. After 10 h the reaction has gone to near completion, with a 23±1 Å layer of oleic acid ($\rho=-0.2\pm0.15\times10^{-6}$ Å^{-2}) remaining on the surface at a volume fraction of 0.55±0.05 and a 21±1 Å thick layer of PLA_2 with an increased volume fraction of 0.5±0.05 (Table 3).

To support our data modeling, we also calculated the reflectivity profiles for the situation where both reaction products leave the interface at equal rates and the chain region scattering length density remains at $3.17\pm0.15\times10^{-6}$ Å^{-2}. The solid red and blue lines in Fig. 6 represent the reflectivities at the same areas per lipid chain as the black lines for 70 and 610 min after the start of the reaction and demonstrate the sensitivity of

Table 2
d_{31}-POPC bilayer before and after *Naja mossambica mossambica* PLA_2 hydrolysis

Lipid	Layer	$\rho/10^{-6}$Å^{-2}*	$\rho_a/10^{-6}$ Å$^{-2\dagger}$	t/Å‡	$\phi^{\P}$	A/Å$^{2\|\|}$	Γ/mg m$^{-2\|\|}$
d_{31}-POPC	Head	1.86±0.15	3.03±0.23	6±1	0.74±0.05	72±20	3.51±0.35
	Chains	3.17±0.15	3.74±0.1	32±2	0.82±0.05	71±7	
cobra PLA_2 **	Head 1§	1.86±0.15	3.61±0.23	4±1	0.61±0.05	132±57	1.91±0.19
70 min.	Chains	1.44±0.15	3.35±0.1	23±2	0.61±0.05	133±17	
	Head 2	2.56±0.15	4.04±0.23	4±1	0.61±0.05	132±57	
	PLA_2	3.61±0.15	5.25±0.2	22±3	0.40±0.05	1760±580	2.50±0.25
cobra PLA_2 **	Head 1§	1.86±0.15	3.70±0.23	4±1	0.59±0.05	137±60	1.85±0.19
140 min.	Chains	1.20±0.15	3.00±0.1	21±2	0.65±0.05	137±19	
	Head 2	2.64±0.15	4.16±0.23	4±1	0.59±0.05	137±60	
	PLA_2	3.61±0.15	5.12±0.2	23±3	0.45±0.05	1490±460	2.94±0.29
cobra PLA_2 **	Head 1§	1.86±0.15	3.75±0.23	4±1	0.58±0.05	139±61	1.82±0.18
210 min.	Chains	0.95±0.15	3.06±0.1	22±2	0.61±0.05	139±19	
	Head 2	2.68±0.15	4.22±0.23	4±1	0.58±0.05	139±61	
	PLA_2	3.61±0.15	5.06±0.2	21±3	0.47±0.05	1570±600	2.80±0.28
cobra PLA_2 **	Oleic acid	0.19±0.15	3.58±0.13	23±2	0.5±0.05	80±11	0.27±0.03
610 min.	PLA_2	3.61±0.15	4.98±0.2	22±3	0.5±0.05	1600±505	2.5±0.25

$^{\dagger}\rho_a$=*fitted* total scattering length density of layer a, including water and/or PLA_2. $^{\P}\phi$ =lipid volume fraction derived from the fitted value of $^{\dagger}\rho_a$. Other symbols are given in the legend of Table 1.

Table 3
Structural parameters of d_{31}-POPC during porcine pancreatic PLA_2 hydrolysis

Lipid	Layer	$\rho/10^{-6}$Å^{-2}	$\rho_a/10^{-6}$Å^{-2}	t/Å	ϕ	A_a/Å^2	Γ/mg m^{-2}
d_{31}-POPC	Heads	1.86±0.15	3.52±0.22	6±1	0.63±0.10	85±31	2.95±0.30
	Chains	3.17±0.25	3.87±0.10	28±2	0.78±0.20	86±25	
pig PLA_2 1 h	Head 1	1.86±0.15	3.84±0.22	6±1	0.56±0.10	96±37	2.49±0.25
	Chains	3.17±0.25	3.77±0.10	24±2	0.81±0.20	96±30	
	Head 2+PLA_2 [#]	2.16±0.15	4.34±0.21	6±1	0.56±0.10	96±30	
	PLA_2 [§]	3.84±0.15	6.22±0.18	21±3	0.05±0.05	14,700±11000	0.30±0.03
pig PLA_2 5 h	Head 1	1.86±0.15	3.66±0.24	5±1	0.60±0.10	107±46	2.34±0.23
	Chains	3.17±0.25	3.97±0.10	23±2	0.75±0.20	108±35	
	Chains+PLA_2 [#]	3.26±0.25	4.03±0.10	5±1	0.75±0.20	108±35	
	Head 2+PLA_2 [#]	2.26±0.15	3.90±0.20	5±1	0.60±0.10	107±46	
	PLA_2	3.84±0.15	5.97±0.18	19±3	0.15±0.05	5400±2600	0.81±0.08
pig PLA_2 10 h	Head 1	1.86±0.15	3.33±0.23	4±1	0.67±0.10	120±61	2.09±0.21
	Chains	2.75±0.25	3.58±0.10	20±2	0.77±0.20	121±41	
	Chains+PLA_2 [#]	3.02±0.25	3.79±0.10	5±1	0.77±0.20	121±41	
	Head 2+PLA_2 [#]	2.24±0.15	3.60±0.21	4±1	0.67±0.10	120±61	
	PLA_2 [§]	3.84±0.15	5.85±0.18	20±3	0.20±0.05	3800±1900	1.14±0.11

[#]PLA_2I initially penetrates into the outer headgroups and after 5 hours, 5Å into the hydrocarbon region. Other symbols are given in the legend of Table 1.

neutron reflection to the layer composition. It was not possible to fit the data using a model assuming an even distribution of the products at any area per molecule, and hence we conclude that the lyso-lipid leaves the surface at the same rate as it is generated by PLA_2. A schematic model for a possible PLA_2 interaction with the POPC bilayer is shown in Fig. 7. Our data points strongly to a mechanism in which the fatty acid accumulation at the interface is accompanied by an increased adsorption of PLA_2 while the lyso-lipid leaves the supported bilayer.

4.4. Distribution of products during the lag phase

We repeated the experiment using d_{31}-POPC with porcine pancreatic PLA_2. The reflectivity profiles in Fig. 8 show that in this case too, only small changes in reflectivity occur during the reaction. Taking into account the possible changes in lipid scattering length density, we interpreted these results using a similar model as for the lag phase of pancreatic PLA_2 with DOPC. The reflectivity profiles indicate that at least a 5-h induction period exists before any significant amount (>10%) of the lipid material begins to leave the membrane. The interaction with PLA_2 leads mainly to thinning of the d_{31}-POPC hydrocarbon region by 4±1 Å. The contrast is less sensitive to the exact location of PLA_2 due to the partial deuteration of the lipid (the chain scattering length density is very close to that of PLA_2), but it was still possible to identify a 21±3 Å layer of the enzyme partially embedded in the bilayer. Even after 5 h the changes in lipid volume fraction remain small, but begin to be accompanied by a slow decrease in the chain scattering length density from 3.17×10^{-6} Å^{-2} to 2.75×10^{-6} Å^{-2}, which implies that some of the deuterated lyso-palmitoyl lipid has left the membrane. Based on the phospholipid component volumes [53],

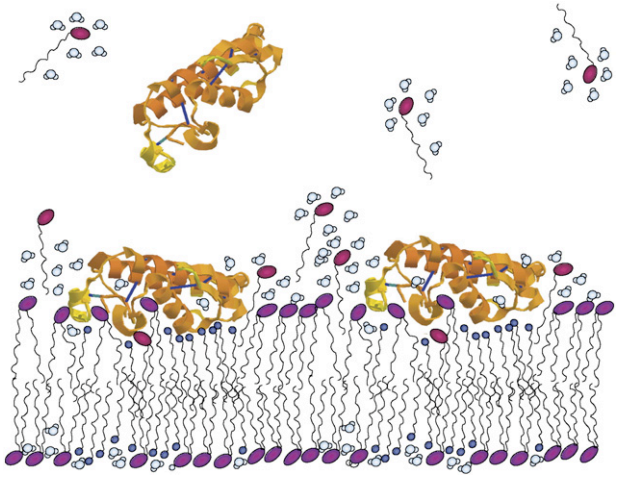

Fig. 7. Schematic model of a possible PLA_2 interaction with a phospholipid bilayer based on the box models used to fit neutron reflectivity data as presented in Table 2. The enzyme resides at the lipid–water interface and partially penetrates into the bilayer. Fatty acid (small blue head group) accumulates in the bilayer as the lyso-phospholipid (large red head group) partitions into the solution.

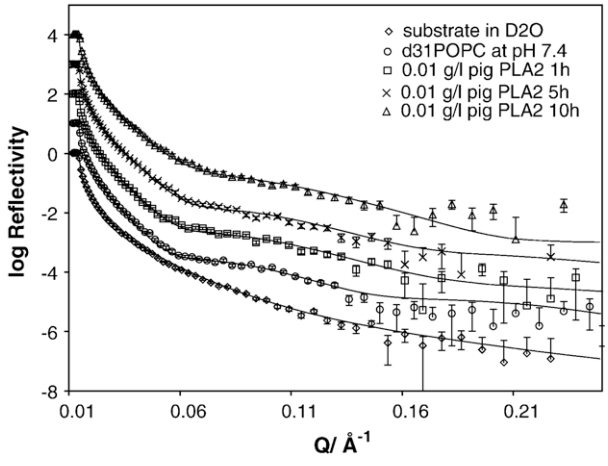

Fig. 8. Specular reflectivity of a supported d_{31}-POPC bilayer at the Silica–D_2O interface recorded before and during porcine pancreatic PLA_2 hydrolysis. (Open diamonds) substrate reflectivity in D_2O, (open circles) d_{31}-POPC bilayer at in 10 mM Tris–D_2O pH 7.4, (open squares) d_{31}-POPC bilayer 1 h after injection of 0.01 mg/ml PLA_2, (crosses) d_{31}-POPC bilayer 5 h after PLA_2 injection and (open triangles) d_{31}-POPC bilayer 10 h after PLA_2 injection. The data fits correspond to the bilayer properties given in Table 3.

we estimate this fraction to be 5% of the deuterated *sn*-1 chains. Although the interfacial PLA_2 volume fraction is initially lower for d_{31}-POPC, it increases even more dramatically during the lag period than was the case for DOPC (Table 4).

4.5. Hydrolysis of DPPC by pancreatic PLA_2

The interaction of pancreatic PLA_2 with DPPC at the same temperature (25 °C) is markedly different from DOPC and POPC. Fig. 9 shows the reflectivity profiles from a chain-deuterated d_{62}-DPPC recorded before and after injection of PLA_2. The bilayer reflectivity was measured in two contrasts, D_2O and water contrast matched to bulk silicon (CmSi, sld = 2.07×10^{-6} Å^{-2}), in order to determine the lipid volume fraction prior to PLA_2 injection. In this case the lipid bilayer had a relatively low volume fraction of only 45% indicating the presence of large (nm-size) lipid-free areas of the support surface, likely to be the result of defects in the underlying surface. The injection of PLA_2 was found to lead to a small increase in reflectivity, which is contrary to what would be expected for a phospholipid bilayer replaced by the solvent (D_2O), and the data were found to fit best to a model in which PLA_2 penetrates uniformly throughout the bilayer but does not catalyze any significant amount of hydrolysis. In a manner similar to DOPC and POPC, the DPPC bilayer becomes 4±1 Å thinner upon interaction with PLA_2 indicating that some enzyme–lipid binding and changes in the lipid packing occur. PLA_2 is likely to bind to the membrane edges around the defects as well as on the top of the membrane, which would make it appear as though it was penetrating deeper into the lipid bilayer. When the DPPC experiment was repeated with a high quality d_{75}-DPPC (chain and head deuterated) bilayer (data not shown), no changes in the bilayer composition were observed over extended periods of time (7 h) even using a 2-fold increase in the enzyme concentration. We also repeated the experiment using a single-chain deuterated d_{31}-DPPC (at 67% volume fraction), but observed no reactivity up to 16 h after PLA_2 injection. These results indicate that this enzyme is inactive towards a DPPC at 25 °C, when it is in the gel state, but also point to the importance of the lipid surface coverage in interpreting results of experiments using supported model membranes. It has been argued by several researchers that PLA_2 can be activated by defects in model membranes [10,11], but our data points to the opposite conclusion; it appears that at 25 °C in the absence of Ca^{2+} DPPC is not hydrolysed by pancreatic PLA_2 even when the bilayer has a large number of defects. This difference from previously published data could be an effect of the experimental conditions such as the nature of the solid surface (e.g. charge), which may change properties of the lipid bilayer [58]. The silica substrates used here have a much lower negative surface charge than mica surfaces which are typically used in atomic force microscopy [59]. It is possible therefore that the lipid molecules in our case have higher lateral and vertical mobility.

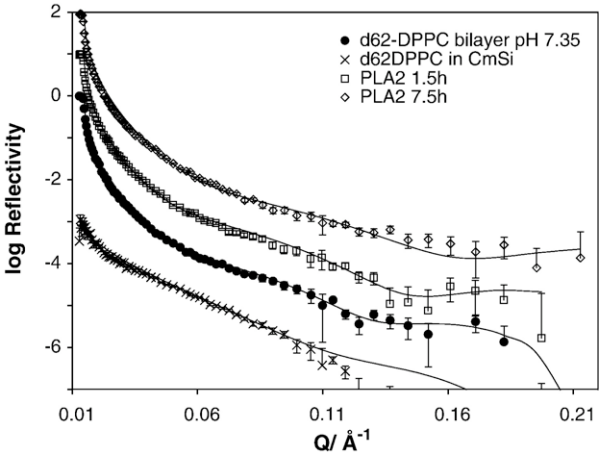

Fig. 9. Specular reflectivity of a supported d_{62}-DPPC bilayer at the Silica–D_2O interface recorded before and during porcine pancreatic PLA_2 hydrolysis. (circles) d_{62}-DPPC bilayer at in 10 mM Tris–D_2O pH 7.4, (crosses) d_{62}-DPPC bilayer at in 10 mM Tris–CmSi pH 7.4, (open squares) d_{62}-DPPC bilayer 1.5 h after injection of 0.01 mg/ml PLA_2, (open diamonds) d_{62}-DPPC bilayer 7.5 h after PLA_2 injection. The data fits correspond to the parameters given in Table 4.

5. Discussion

5.1. Compositional changes and the role of reaction products in PLA_2 activation

Our results constitute the first direct measurement of the absolute amount of PLA_2 bound to a phospholipid bilayer during the lag phase, and show unambiguously that it increases, although the changes observed in lipid composition are small. More remarkable is that in both cases, DOPC and d_{31}-POPC, the lag phase is terminated when 5±3% of the lipid molecules have been hydrolysed although the time required for this is considerably longer for d_{31}-POPC. The volume fraction of

Table 4
Fitted parameters and bilayer properties of d_{62}-DPPC before and during PLA_2 hydrolysis

Lipid	Layer	$\rho/10^{-6}$ Å^{-2}	ϕ(PLA$_2$)	$\rho_a/10^{-6}$ Å^{-2}	t/Å	ϕ	A$_a$/Å^2	Γ/mg m^{-2}
d_{62}-DPPC	Head	1.84±0.25	–	1.97±0.10	7±1	0.44±0.05	106±30	2.29±0.23
CmSi	Chains	6.89±0.15	–	4.24±0.10	37±2	0.45±0.02	107±11	
d_{62}-DPPC	Head	1.84±0.15	–	4.37±0.23	7±1	0.44±0.05	106±30	2.29±0.23
D_2O TRIS pH 7.4	Chains	6.89±0.25	–	6.59±0.11	37±2	0.45±0.2	107±41	
pig PLA_2 #	Head	2.14±0.15	0.15±0.08	4.03±0.21	7±1	0.55±0.05	85±22	2.88±0.29
0.01 g/l 1.5 h	Chains	6.43±0.25	0.15±0.08	6.41±0.11	30±2	0.70±0.20	85±26	
pig PLA_2 #	Head	2.24±0.15	0.20±0.08	3.88±0.21	6±1	0.60±0.05	91±27	2.68±0.62
0.01 g/l 7.5 h	Chains	6.28±0.25	0.20±0.08	6.30±0.11	26±2	0.75±0.20	91±28	

Symbols are given in the legend of Table 1.

PLA_2 bound to d_{31}-POPC is initially higher but in both cases it increases by ~5 vol.% during the course of the lag phase, indicating that the departure of the lyso-PC and generation of fatty acid enhance PLA_2 binding to the membrane.

These results are in good agreement (to within our experimental error of ±3 vol.%) with the critical product mole fraction of 8.3% found in previous studies [11] to be sufficient to eliminate the lag phase of pancreatic PLA_2. Our results also show that despite the lyso-lipid being a leaving group in the membrane, its structure has an effect on the activation of PLA_2 by way of regulating the length of the lag phase. Under conditions where the lag phase has been eliminated by addition of Ca^{2+}, the effect of the lyso-lipid on the initial rate of PLA_2 hydrolysis has been found to be much smaller than that of the fatty acid [60]. Considered together with the evidence from our experiment that the enzyme seems to be inactive towards, but still interacts with DPPC in the gel-state, this suggests that the PLA_2–membrane interaction has two steps, adsorption of the enzyme to the lipid–water interface and subsequent penetration to the lipid hydrocarbon core, the latter being required for catalytic activity. The amount of the enzyme bound to the lipid interface initially was found to be very similar for DOPC and DPPC with both pancreatic and cobra venom PLA_2 at 25 °C, which suggests that it is predominantly driven by electrostatic interactions with the headgroup, but that the penetration step, which is required for catalytic activity, is more dependent on the nature of the phospholipid packing, and hence, the nature of the *sn*-1 chain. These effects may even be coupled to each other due to the difference in lipid conformation in the fluid and gel phase. For example MAS-NMR studies [61] have shown that the $^{31}P–^{14}N$ dipole in phosphocholine headgroups is almost parallel to the lipid–water interface in fluid membranes, whereas it is more perpendicular to the interface in the gel state, in which case the negative charge of the phosphate (and acyl bonds) may be effectively shielded by the positively charged choline nitrogen. This means that ultimately PLA_2 activity is sensitive to both hydrophobic and electrostatic interactions between the lipids and the enzyme and these all determine whether it can access the acyl bonds to be hydrolysed and release the products in order to continue the catalytic cycle.

Our results are also the first direct measurement of membrane compositional changes during active PLA_2 hydrolysis. The solution partitioning of the d_{31}-lyso-lipid and the accumulation of fatty acid in the membrane are consistent with the solubilities of the two reaction products, with the lyso-lipid having a large zwitterionic head group and the fatty acid a long saturated hydrocarbon chain. Although lyso-lipids and fatty acids can form planar bilayer structures when present in a 1:1 ratio, when they are generated in the membrane there will be an equilibrium between the membrane and the aqueous phase leading to a partitioning of each according to their solubilities. The cmc of 1-palmitoyl-3-*sn*-phosphocholine is 70 μM [62] which is considerably higher than the entire stock of lysolipid that can be released from the supported membrane into the solution and this acts as a driving force for its solubilisation from the membrane. For example, in our bilayers, d_{31}-POPC has an average available molecular are of $A_{mol}=72$ Å^2, and the surface of our silicon crystal is 5000 mm^2, which accommodates 6.94×10^{15} molecules = 11 nmol. This would give rise to a concentration of 0.5 μM in a 22-ml neutron reflectivity cell, which is 140 times smaller than the cmc of lyso-palmitoyl-PC. The C18:1 fatty acid is orders of magnitude less soluble. The possibility of reaction product retention in the hydrolysis of short chain lipid monolayers has been suggested [63], but ours is the first confirmation of the changing lipid composition and the almost exclusive solubilisation of the C16:0-lyso-PC.

An increased interaction of the enzyme with reaction products in the membrane has been postulated before [11,15,64,65], and has, in the absence of methods to quantify the interfacial product concentrations, been a subject of much speculation. In simple terms the product activation can be understood as an increased electrostatic interaction arising from the presence of (at pH 7.4) negatively charged fatty acids with the enzyme, which is known to have several cationic residues that participate in the membrane interaction [66,67]. Thus, the enzyme partitioning is shifted towards the membrane bound state with increasing fatty acid content of the membrane. That this effect varies so much between three lipids as closely related as DOPC, POPC and DPPC, suggests that the reactivity of pancreatic PLA_2 also dramatically depends on the lipid chain packing.

A debate about the mechanism of PLA_2 activation has been going on for decades between the leading groups in the area. While the Jain group postulates that the activation is solely based on electrostatic interactions, i.e. that only the number of enzymes adsorbed at the membrane interface counts [63], the Verger laboratory originally suggested that a penetration step is also required [68]. It is interesting to compare the implications of these concepts in light of the results from our experiments. Our results support the product activation hypothesis by confirming that the amount of PLA_2 at the interface increases during the lag phase (pancreatic PLA_2), and also during the active phase (cobra PLA_2). However, if the activation of PLA_2 were only dependent on the initial electrostatic interactions, then the length of the lag phase should be the same for all phosphatidylcholine bilayers, because the amount of enzyme initially adsorbed is remarkably similar for all three lipids. However, we see a significant difference in the lag length even between DOPC (3 h) and POPC (5 h) and no catalytic activity towards DPPC, which clearly suggests that the activation involves another rate limiting step. Jain et al. suggest that the negative fatty acid accumulation would only activate the initial enzyme adsorption step and increase k^*_{cat}, the rate constant of the catalytic conversion step, but the parameters used by Jain et al. are derived from the kinetic analysis of homogenous catalysis and cannot be used to describe the changes in the membrane structure that can also occur due to the reaction product accumulation, such as increased/decreased fluidity, interfacial roughness or lateral heterogeneity. The penetration scheme of Verger has been impossible to validate in the absence of methods to measure the penetration directly.

We believe that our neutron reflection and ellipsometry results offer the first confirmation and a possible explanation of several previously predicted effects. Our earlier results already indicated that the location of PLA_2 in supported bilayers

overlaps with the lipid headgroups, and part of the outer leaflet chain region [44]. Accompanying the lag phase we have now also observed an increase in the penetration depth of PLA_2. Both results strongly support the idea of a penetration step as rate limiting in catalytic activity. Thirdly, we see a similar amount of PLA_2 adsorbed on the inactive DPPC bilayer during the lag phase as on the active DOPC bilayer during hydrolysis. Therefore the enzyme adsorption step cannot be the single activating process.

At least two different modes of membrane binding have been identified for PLA_2 by fluorescence spectroscopy [6,7]. While there is no direct structural evidence for a conformational change of the enzyme, it is more certain that the different fluorescence states represent two different types of PLA_2–lipid interactions, i.e. two different locations of the enzyme at the lipid–water interface. Penetration into the lipid chain region implies that the lipids are also required to have the conformational freedom to allow PLA_2 to reach its *catalytic depth* as a part of lipid insertion into the active site. This catalytic depth could be described as the location in which all hydrophobic and electrostatic enzyme–lipid–water interactions are optimized, and may be very sensitive to the surface features of the enzyme and the lipid conformation. Thus an inactive form of PLA_2 could be bound at the lipid–water interface without being able to perform catalysis, which would explain the apparent inactivity of porcine pancreatic PLA_2 towards DPPC (in the absence of electrolytes) at 25 °C. The inactivity would be expected to disappear when the lipids are heated to near or above the phase transition temperature, as has indeed been observed in DPPC vesicles [14], which are inactive towards pancreatic PLA_2 in the absence of Ca^{2+} but exhibit a substrate concentration dependent lag-burst behavior similar to unsaturated lipids above 38 °C. The importance of lipid conformation is further supported by results obtained from liquid chromatographic separations of lipid mixtures such as DMPC/DSPC, in which the fluid lipid is preferentially hydrolysed [69].

It has also been suggested [11,24] that the presence of reaction products causes phase separation in the membrane and can activate PLA_2 via defects. Given the complete solubilisation of the lyso-lipid evident in our neutron reflectivity data, this effect would then be solely due to the fatty acids, which can have very different properties according to the nature of their hydrocarbon chain. In particular it has been found that the effect of unsaturated fatty acids on a phospholipid bilayer structure is negligible compared to saturated fatty acids [70]. A saturated long chain fatty such as palmitic acid tends to pack tightly into a crystalline lattice even at physiological temperatures, while the corresponding unsaturated fatty acid is much more flexible and has virtually no effect on the lipid bilayer melting temperature. The increased binding of PLA_2 to the d_{31}-POPC bilayer with increasing oleic acid content confirms that the binding of this enzyme is favored by the accumulating fatty acid, but the strength of their interaction does not inhibit catalysis, which proceeds to near completion. However, hydrolysis of DPPC by *Naja m. mossambica* PLA_2 stops after only ~15% of the phospholipid has been consumed, although PLA_2 is still found to be present in the inactive membrane. This behavior can only be explained by a binding interaction which has become so strong that the catalytic cycle of PLA_2 is disrupted and the enzyme is irreversibly bound to the lipid matrix. Such trapping could be caused by tightly packed domains of palmitic acid. The reversibility of PLA_2 binding to model lipid interfaces has been a matter of interest for some decades, mainly due to the influence it has on the types of kinetic analyses that can be applied, with the "scooting" and "hopping" modes being referred to as the irreversible and reversible cases respectively [71]. The apparent deactivation or trapping of PLA_2 in DPPC membranes suggests that the binding in this case at least is irreversible, as otherwise the enzyme could continue the reaction by "hopping" in and out of the membrane. It also suggests that the effect of the fatty acids is local substrate depletion because the reaction stops at such an early stage.

Our results are consistent with results on *Agkistrodon piscivorus piscivorus* (Type IIA [1]) PLA_2 hydrolysis obtained by Tatulian et al. [72] using attenuated total reflection infra-red spectroscopy (ATR-FTIR) [73], where the hydrolysis of *sn*-1 deuterated DPPC was followed by monitoring the integrated CH_2 and CD_2 vibration intensities. A 20% difference in the fraction of unlabelled and labelled acyl chains retained in the membrane was observed by Tatulian et al., which is relatively small compared to the complete elimination of the lyso-lipid that we measured for d_{31}-POPC and pancreatic PLA_2, but does correlate well with our results on DPPC hydrolysis by *Naja mossambica mossambica* PLA_2 (which exhibits no lag phase). It may be that the variation is a result of different lipid–enzyme interactions of the three different PLA_2s. In Tatulian's case the *Agistrodon piscivorus piscivorus* PLA_2 (which does exhibit a lag phase in the absence of Ca^{2+}) was also activated by 2 mM $CaCl_2$, whereas we used no Ca^{2+} in our experiments. The similarity of results for the two active enzymes is interesting because the enzymes belong to two different classes but the total amount of lipid hydrolysed is in close agreement.

Overall, our results are contradictory to the assumptions used in the scooting model of interfacial hydrolysis, in that the membrane composition changes on both sides of the supported bilayer, implying that flip-flop of the fatty acid/phospholipid [74] is readily achieved without penetration of PLA_2 to the other side of the bilayer. Although supported bilayers and vesicles differ in some of their properties as model membranes, the evidence presented for the integrity of vesicles during lipid hydrolysis by Jain et al. is inconclusive, especially when considered in the light of the now measured solubilisation of the lyso-lipids. Virtually all the PLA_2 hydrolysis data used to formulate the scooting model has been generated indirectly by sampling the entire reaction mixture or by measuring pH. In fact a temperature dependent release of fluorescence markers during PLA_2 hydrolysis has been observed in phosphocholine vesicles [21,69], and it could be due to the slow removal of the lyso-lipids. The only other evidence for the scooting model is that the total amount of lipid material hydrolysed [75] correlates with the amount of lipid assumed to reside in the outer leaflet of the vesicles based on the average size. The extent of hydrolysis in solution is most commonly measured by pH-Stat titrations [71], but it has previously been commented that rapid flip-flop of the

fatty acids to the interior of the vesicles can give rise to misleading results [76,77]. We would therefore like to speculate that the end-point of hydrolysis is not necessarily achieved when all the outer lipids have been digested, but when the outer lipid–product mixture has reached a limiting composition in which PLA_2 can no longer effectively catalyse hydrolysis. The main concern with using the scooting model to interpret the so-called "interfacial processivity" of enzymes is however that it only applies to negatively charged micelle or (small unilamellar) vesicle interfaces, which often contain non-naturally occurring components, such as phosphomethanol lipids or detergents. Such highly curved and highly charged interfaces are hardly similar to the natural operating environment of PLA_2, which may exhibit comparatively different behavior towards cell membranes.

6. Conclusion

By using neutron reflection we have determined the composition of supported lipid bilayer during PLA_2 hydrolysis and the lag phase of pancreatic PLA_2 in situ together with the amount and location of membrane-bound PLA_2. The increase in the amount of PLA_2 bound to both DOPC and d_{31}-POPC during the lag phase strongly supports the idea that the lag phenomenon is a result of gradual changes in the lipid matrix that lead to an enhancement of PLA_2 affinity for the membrane. An increase in the penetration depth of PLA_2 into the d_{31}-POPC bilayer is observed before the start of rapid hydrolysis, indicating that the accumulation of reaction products also facilitates the hydrophobic interaction between the lipid chains and the enzyme that leads to its activation. The changes in the neutron reflectivity profile of d_{31}-POPC compared to POPC indicate unambiguously that the scattering length density of the partially deuterated membrane decreased during the reaction and all data profiles could be fitted using a model of gradual removal of the deuterated lyso-C16-PC from the bilayers.

The exact mechanism of phospholipase A_2 hydrolysis remains elusive, but our results demonstrate for the first time the actual fate of the reaction products and show that PLA_2 is highly sensitive to the lipid chain composition, which calls for the development of more accurate kinetic analyses to describe the effects of the reaction products. The biological functions and substrates of PLA_2 are diverse, and it is likely that its regulation is related to the membrane lipid composition in each environment. Since PLA_2 plays a major role in inflammatory response, it is a good candidate for drug development aimed at its selective inhibition [78], but advance is hampered by a lack of understanding about the subtleties of its regulation. We have shown that neutron reflection gives unique information about the composition and structure of phospholipid membranes, and is a valuable tool in studying the regulation of membrane binding enzymes such as PLA_2.

Acknowledgements

This work was supported by the UK Biotechnology and Biological Sciences Research Council (BBSRC), the EU Marie Curie training network, the Academy of Finland and the Finnish Cultural Foundation. The authors would like to thank Dr. John Webster of the ISIS Neutron Facility, UK for his help in the realization of these experiments.

References

[1] D.A. Six, E.A. Dennis, The expanding superfamily of phospholipase A(2) enzymes: classification and characterization, Biochim. Biophys. Acta-Mol. Cell Biol. Lipids 1488 (2000) 1–19.
[2] R.K. Arni, R.J. Ward, Phospholipase A(2)—A structural review, Toxicon 34 (1996) 827–841.
[3] B.W. Dijkstra, J. Drenth, K.H. Kalk, Active-site and catalytic mechanism of phospholipase-A2, Nature 289 (1981) 604–606.
[4] D.L. Scott, S.P. White, Z. Otwinowski, W. Yuan, M.H. Gelb, P.B. Sigler, Interfacial catalysis—The mechanism of phospholipase-A2, Science 250 (1990) 1541–1546.
[5] M.H. Gelb, J.H. Min, M.K. Jain, Do membrane-bound enzymes access their substrates from the membrane or aqueous phase: interfacial versus non-interfacial enzymes, Biochim. Biophys. Acta-Mol. Cell Biol. Lipids 1488 (2000) 20–27.
[6] W.R. Burack, M.E. Gadd, R.L. Biltonen, Modulation of phospholipase a (2)—Identification of an inactive membrane-bound state, Biochemistry 34 (1995) 14819–14828.
[7] M.E. Gadd, R.L. Biltonen, Characterization of the interaction of phospholipase A(2) with phosphatidylcholine-phosphatidylglycerol mixed lipids, Biochemistry 39 (2000) 9623–9631.
[8] J.D. Bell, R.L. Biltonen, Molecular details of the activation of soluble phospholipase- A(2) on lipid bilayers—Comparison of computer-simulations with experimental results, J. Biol. Chem. 267 (1992) 11046–11056.
[9] L.K. Nielsen, J. Risbo, T.H. Callisen, T. Bjornholm, Lag-burst kinetics in phospholipase A(2) hydrolysis of DPPC bilayers visualized by atomic force microscopy, Biochim. Biophys. Acta-Biomembr. 1420 (1999) 266–271.
[10] T. Honger, K. Jorgensen, R.L. Biltonen, O.G. Mouritsen, Systematic relationship between phospholipase A(2) activity and dynamic lipid bilayer microheterogeneity, Biochemistry 35 (1996) 9003–9006.
[11] W.R. Burack, Q. Yuan, R.L. Biltonen, Role of lateral phase-separation in the modulation of phospholipase-A2 activity, Biochemistry 32 (1993) 583–589.
[12] R. Verger, M.C.E. Mieras, G.H. de Haas, Action of phospholipase A at interfaces, J. Biol. Chem. 218 (1973) 4023–4034.
[13] S.A. Tatulian, R.L. Biltonen, L.K. Tamm, Structural changes in a secretory phospholipase A(2) induced by membrane binding: a clue to interfacial activation? J. Mol. Biol. 268 (1997) 809–815.
[14] G. Romero, K. Thompson, R.L. Biltonen, The activation of porcine pancreatic phospholipase-A2 by dipalmitoylphosphatidylcholine large unilamellar vesicles—Analysis of the state of aggregation of the activated enzyme, J. Biol. Chem. 262 (1987) 13476–13482.
[15] R. Apitzcastro, M.K. Jain, G.H. Dehaas, Origin of the latency phase during the action of phospholipase- A2 on unmodified phosphatidylcholine vesicles, Biochim. Biophys. Acta 688 (1982) 349–356.
[16] J. Davidsen, O.G. Mouritsen, K. Jorgensen, Synergistic permeability enhancing effect of lysophospholipids and fatty acids on lipid membranes, Biochim. Biophys. Acta-Biomembr. 1564 (2002) 256–262.
[17] Y. Cajal, M.K. Jain, Synergism between mellitin and phospholipase A(2) from bee venom: apparent activation by intervesicle exchange of phospholipids, Biochemistry 36 (1997) 3882–3893.
[18] R. Verger, G.H.D. Haas, Enzyme reactions in a membrane model: 1. New technique to study enzyme reactions in monolayers, Chem. Phys. Lipids 10 (1973) 127–136.
[19] E.A. Dennis, Kinetic dependence of phospholipase A2 activity on detergent triton X-100, J. Lipid Res. 14 (1973) 152–159.
[20] M.K. Jain, J. Rogers, D.V. Jahagirdar, J.F. Marecek, F. Ramirez, Kinetics of interfacial catalysis by phospholipase A2 in intravesicle scooting mode, and heterofusion of anionic and zwitterionic vesicles, Biochim. Biophys. Acta 860 (1986) 435–447.
[21] O.G. Berg, B.Z. Yu, J. Rogers, M.K. Jain, Interfacial catalysis by

phospholipase-A2—Determination of the interfacial kinetic rate constants, Biochemistry 30 (1991) 7283–7297.
[22] G.M. Carman, R.A. Deems, E.A. Dennis, Lipid signaling enzymes and surface dilution kinetics, J. Biol. Chem. 270 (1995) 18711–18714.
[23] I. Panaiotov, R. Verger, in: A. Baszkin, W. Norde (Eds.), Physical Chemistry of Biological Interfaces, Marcel Dekker Inc., New York, 2000, pp. 359–400.
[24] K.M. Maloney, M. Grandbois, D.W. Grainger, C. Salesse, K.A. Lewis, M.F. Roberts, Phospholipase A(2) domain formation in hydrolyzed asymmetric phospholipid monolayers at the air/water interface, Biochim. Biophys. Acta-Biomembr. 1235 (1995) 395–405.
[25] J.B. Hayter, R.R. Highfield, B.J. Pullman, R.K. Thomas, A.I. McMullen, J. Penfold, Critical reflection of neutrons—A new technique for investigating interfacial phenomena, J. Chem. Soc.-Faraday Trans. I 77 (1981) 1437–1448.
[26] G. Fragneto-Cusani, Neutron reflectivity at the solid/liquid interface: examples of applications in biophysics, J. Phys.-Condens. Matter 13 (2001) 4973–4989.
[27] T. Gutberlet, R. Steitz, G. Fragneto, B. Klosgen, Phospholipid bilayer formation at a bare Si surface: a time-resolved neutron reflectivity study, J. Phys.-Condens. Matter 16 (2004) S2469–S2476.
[28] S. Krueger, Neutron reflection from interfaces with biological and biomimetic materials, Curr. Opin. Colloid Interface Sci. 6 (2001) 111–117.
[29] B. Stidder, G. Fragneto, R. Cubitt, A.V. Hughes, S.J. Roser, Cholesterol induced suppression of large swelling of water layer in phosphocholine floating bilayers, Langmuir 21 (2005) 8703–8710.
[30] U.A. Perez-Salas, K.M. Faucher, C.F. Majkrzak, N.F. Berk, S. Krueger, E.L. Chaikof, Characterization of a biomimetic polymeric lipid bilayer by phase sensitive neutron reflectometry, Langmuir 19 (2003) 7688–7694.
[31] C.A. Naumann, O. Prucker, T. Lehmann, J. Ruhe, W. Knoll, C.W. Frank, The polymer-supported phospholipid bilayer: tethering as a new approach to substrate–membrane stabilization, Biomacromolecules 3 (2002) 27–35.
[32] G. Fragneto, F. Graner, T. Charitat, P. Dubos, E. Bellet-Amalric, Interaction of the third helix of Antennapedia homeodomain with a deposited phospholipid bilayer: a neutron reflectivity structural study, Langmuir 16 (2000) 4581–4588.
[33] C.E. Miller, J. Majewski, K. Kjaer, M. Weygand, R. Faller, S. Satija, T.L. Kuhl, Neutron and X-ray scattering studies of cholera toxin interactions with lipid monolayers at the air–liquid interface, Colloids Surf., B 40 (2005) 159–163.
[34] C.P. Johnson, G. Fragneto, O. Konovalov, V. Dubosclard, J.F. Legr, D.E. Leckband, Structural studies of the neural-cell-adhesion molecule by X-ray and neutron reflectivity, Biochemistry 44 (2005) 546–554.
[35] E. Sackmann, Supported membranes: scientific and practical applications, Science 271 (1996) 43–48.
[36] F. Tiberg, I. Harwigsson, M. Malmsten, Formation of model lipid bilayers at the silica–water interface by co-adsorption with non-ionic dodecyl maltoside surfactant, Eur. Biophys. J. Biophys. Lett. 29 (2000) 196–203.
[37] H. Vacklin, F. Tiberg, R.K. Thomas, Formation of supported phospholipid bilayers via co-adsorption with b-D-dodecyl maltoside, Biochim. Biophys. Acta—Biomembr. 1668 (2005) 17–24.
[38] H. Vacklin, F. Tiberg, G. Fragneto, R.K. Thomas, Composition of supported model membranes determined by neutron reflection, Langmuir 21 (2005) 2827–2837.
[39] T. Brumm, C. Naumann, E. Sackmann, A.R. Rennie, R.K. Thomas, D. Kanellas, J. Penfold, T.M. Bayerl, Conformational-changes of the lecithin headgroup in monolayers at the air/water interface—A neutron reflection study, Eur. Biophys. J. Biophys. Lett. 23 (1994) 289–295.
[40] C. Naumann, T. Brumm, A.R. Rennie, J. Penfold, T.M. Bayerl, Hydration of DPPC monolayers at the air/water interface and its modulation by the nonionic surfactant C(12)E(4)—A neutron reflection study, Langmuir 11 (1995) 3948–3952.
[41] C. Naumann, C. Dietrich, A. Behrisch, T. Bayerl, M. Schleicher, D. Bucknall, E. Sackmann, Hisactophilin-mediated binding of actin to lipid lamellae: a neutron reflectivity study of protein membrane coupling, Biophys. J. 71 (1996) 811–823.
[42] C. Naumann, C. Dietrich, J.R. Lu, R.K. Thomas, A.R. Rennie, J. Penfold, T.M. Bayerl, Structure of mixed monolayers of dipalmitoylglycerophosphocholine and polyethylene-glycol monododecyl ether at the air–water-interface determined by neutron reflection and film balance techniques, Langmuir 10 (1994) 1919–1925.
[43] R.M.A. Azzam, N.M. Bashara, Ellipsometry and Polarised Light, North-Holland, Amsterdam, 1986.
[44] H. Vacklin, F. Tiberg, G. Fragneto, R.K. Thomas, Phospholipase A2 hydrolysis of supported phospholipid bilayers: a neutron reflectivity and ellipsometry study, Biochemistry 44 (2005) 2811–2821.
[45] J.E. Bradley, E.M. Lee, R.K. Thomas, A.J. Willatt, J. Penfold, R.C. Ward, D.P. Gregory, W. Waschkowski, Adsorption at the liquid surface studied by means of specular reflection of neutrons, Langmuir 4 (1988) 821–826.
[46] G. Fragneto, Z.X. Li, R.K. Thomas, A.R. Rennie, J. Penfold, A neutron reflectivity study of the adsorption of aerosol-OT on self-assembled monolayers on silicon, J. Colloid Interface Sci. 178 (1996) 531–537.
[47] J.S. Pedersen, I.W. Hamley, Analysis of neutron and X-ray reflectivity data by constrained least-squares methods, Phys., B Condens. Matter 198 (1994) 16–23.
[48] P.N. Thirtle. AFit Simulation Program, v3.1., Oxford University (1997).
[49] M. Landgren, B. Jonsson, Determination of the optical-properties of Si/SiO2 surfaces by means of ellipsometry, using different ambient media, J. Phys. Chem. 97 (1993) 1656–1660.
[50] F. Tiberg, M. Landgren, Characterization of thin nonionic surfactant films at the silica water interface by means of ellipsometry, Langmuir 9 (1993) 927–932.
[51] R. Cubitt, G. Fragneto, D17: the new reflectometer at the ILL, Appl. Phys. A: Mater. Sci. Proc. 74 (2002) S329–S331.
[52] O.S. Heavens, Optical Properties of Thin Films, Butterworths, London, 1955.
[53] H.I. Petrache, S.E. Feller, J.F. Nagle, Determination of component volumes of lipid bilayers from simulations, Biophys. J. 72 (1997) 2237–2242.
[54] R.S. Armen, O.D. Uitto, S.E. Feller, Phospholipid component volumes: determination and application to bilayer structure calculations, Biophys. J. 75 (1998) 734–744.
[55] F.J. Joubert, *Naja Mossambica Mossambica* venom: purifications, some properties and the amino acid sequences of three phospholipases A (CM-I, CM-II and CM-II), Biochim. Biophys. Acta 493 (1977) 216–227.
[56] A.A. Zamyatin, Protein volume in solution, Prog. Biophys. Mol. Biol. 24 (1972) 107–123.
[57] B. Jacrot, Rep. Prog. Phys. 39 (1976) 911.
[58] R.P. Richter, N. Maury, A.R. Brisson, On the effect of the solid support on the interleaflet distribution of lipids in supported lipid bilayers, Langmuir 21 (2005) 299–304.
[59] L.K. Nielsen, K. Balashev, T.H. Callisen, T. Bjornholm, Influence of product phase separation on phospholipase A2 hydrolysis of supported phospholipid bilayers studied by force microscopy, Biophys. J. 83 (2002) 2617–2624.
[60] M.K. Jain, D.V. Jahagirdar, Action of phospholipase-A2 on bilayers—Effect of fatty-acid and lysophospholipid additives on the kinetic-parameters, Biochim. Biophys. Acta 814 (1985) 313–318.
[61] F.W. Lindstroem, P.T.F. Williamson, G. Goebner, Molecular insight into the electrostatic membrane surface potential by 14N/31P MAS NMR spectroscopy: nociception–lipid association, J. Am. Chem. Soc. 127 (2004) 6610–6616.
[62] R.E. Stafford, T. Fanni, E.A. Dennis, Interfacial properties and critical micelle concentration of lysophospholipids, Biochemistry 28 (1989) 5113–5120.
[63] Y. Cajal, M.A. Alsina, O.G. Berg, M.K. Jain, Product accumulation during the lag phase as the basis for the activation of phospholipase A(2) on monolayers, Langmuir 16 (2000) 252–257.
[64] Y. Cajal, O. Berg, M.K. Jain, Origin of delays in monolayer kinetics: phospholipase A2 paradigm, Biochemistry 43 (2004) 9256–9264.
[65] T. Wieloch, B. Borgstrom, G. Pieroni, F. Pattus, R. Verger, Product activation of pancreatic lipase, J. Biol. Chem. 257 (1982) 11523–11528.
[66] Y.H. Pan, T.M. Epstein, M.K. Jain, B.J. Bahnson, Five coplanar anion binding sites on one face of phospholipase A(2). Relationship to interface binding, Biochemistry 40 (2001) 609–617.
[67] B.Z. Yu, M.J. Poi, U.A. Ramagopal, R. Jain, S. Ramakumar, O.G. Berg,

M.D. Tsai, K. Sekar, M.K. Jain, Structural basis of the anionic interface preference and k*(cat) activation of pancreatic phospholipase A(2), Biochemistry 39 (2000) 12312–12323.
[68] R. Verger, M.C.E. Mieras, G.H. Dehaas, Action of phospholipase a at interfaces, J. Biol. Chem. 248 (1973) 4023–4034.
[69] C. Leidy, O.G. Mouritsen, K. Jorgensen, N.H. Peters, Evolution of a rippled membrane during phospholipase A(2) hydrolysis studied by time-resolved AFM, Biophys. J. 87 (2004) 408–418.
[70] T. Inoue, S. Yanagihara, Y. Misono, M. Suzuki, Effect of fatty acids on phase behavior of hydrated dipalmitoylphosphatidylcholine bilayer: saturated versus unsaturated fatty acids, Chem. Phys. Lipids 109 (2001) 117–133.
[71] O.G. Berg, M.K. Jain, Interfacial Enzyme Kinetics, John Wiley & Sons, Ltd., Chichester, 2002.
[72] S.A. Tatulian, Toward understanding interfacial activation of secretory phospholipase A(2) (PLA(2)): membrane surface properties and membrane-induced structural changes in the enzyme contribute synergistically to PLA(2) activation, Biophys. J. 80 (2001) 789–800.
[73] S.A. Tatulian, Attenuated total reflection Fourier transform infrared spectroscopy: a method of choice for studying membrane proteins and lipids, Biochemistry 42 (2003) 11898–11907.
[74] J.a.C. Liu, J.C. Conboy, 1,2-diacyl-phosphatidylcholine flip-flop measured directly by sum-frequency vibrational spectroscopy, Biophys. J. 89 (2005) 2522–2532.
[75] M.K. Jain, J. Rogers, D.V. Jahagirdar, J.F. Marecek, F. Ramirez, Kinetics of interfacial catalysis by phospholipase-A2 in intravesicle scooting mode, and heterofusion of anionic and zwitterionic vesicles, Biochim. Biophys. Acta 860 (1986) 435–447.
[76] F. Kamp, J.A. Hamilton, Ph gradients across phospholipid-membranes caused by fast flip- flop of unionized fatty-acids, Proc. Natl. Acad. Sci. U. S. A. 89 (1992) 11367–11370.
[77] F. Kamp, H.V. Westerhoff, J.A. Hamilton, Movement of fatty-acids, fatty-acid analogs, and bile-acids across phospholipid-bilayers—Kinetics of fatty acid-mediated proton movement across small unilamellar vesicles, Biochemistry 32 (1993) 11074–11086.
[78] S. Yedgar, D. Lichtenberg, E. Schnitzer, Inhibition of phospholipase A(2) as a therapeutic target, Biochim. Biophys. Acta-Mol. Cell Biol. Lipids 1488 (2000) 182–187.